Eur Radiol (2011) 21:1938–1947
DOI 10.1007/s00330-011-2139-x

GASTROINTESTINAL

# 64-section multidetector CT of the upper abdomen: optimization of a saline chaser injection protocol for improved vascular and parenchymal contrast enhancement

**Daniele Marin · Rendon C. Nelson · Antonino Guerrisi · Huiman Barnhart · Sebastian T. Schindera · Roberto Passariello · Carlo Catalano**

Received: 21 January 2011 / Revised: 19 March 2011 / Accepted: 4 April 2011 / Published online: 11 May 2011


**Abstract**
*Objectives* To prospectively investigate the effect of varying the injection flow rates of a saline chaser on vascular and parenchymal contrast enhancement during abdominal MDCT.
*Methods* 100 consecutive patients were randomly assigned to four injection protocols. A fixed dose of contrast medium was administered followed by no saline (Protocol A) or 50 mL of saline at 2, 4, or 8 mL/s (Protocols B, C, and D). Peak, time-to-peak, and duration of 90% peak enhancement were determined for aorta, pancreas, and liver.
*Results* Aortic peak enhancement was significantly higher for Protocol D (369.5 HU) compared with Protocols A and B (332.9 HU and 326.0 HU, respectively; $P<0.05$). Pancreatic peak enhancement was significantly higher for Protocols C and D (110.6 HU and 110.9 HU, respectively) compared to Protocol A (92.5 HU; $P<0.05$). Aortic and pancreatic time-to-peak enhancement occurred significantly later for Protocol D compared with Protocol A (42.8 s vs. 36.1 s [$P<0.001$] and 49.7 s vs. 45.3 s [$P=0.003$]).
*Conclusions* Injecting a saline chaser at high flow rates yields significantly higher peak aortic and pancreatic enhancement, with a slight longer time-to-peak enhancement.

**Keywords** Abdomen · Tomography · Spiral computed · Contrast media · Injections · Intravenous · Extravasation of diagnostic and therapeutic material

D. Marin (✉) · R. C. Nelson
Department of Radiology, Duke University Medical Center,
Erwin Road,
Durham, NC 27710, USA
e-mail: danielemarin2@gmail.com

D. Marin · A. Guerrisi · R. Passariello · C. Catalano
Department of Radiological Sciences,
University of Rome Sapienza,
Viale Regina Elena 324,
Rome 00161, Italy

H. Barnhart
Department of Biostatistics and Bioinformatics,
Duke University Medical Center,
Durham, NC 27710, USA

S. T. Schindera
Institute for Diagnostic, Interventional and Pediatric Radiology,
University Hospital of Bern,
Bern, Switzerland

## Introduction

The rapid intravenous injection of a bolus of saline following the administration of iodinated contrast material — often referred to as the saline chaser technique — has become standard practice for many abdominal multi-detector row computed tomography (MDCT) injection protocols [1, 2]. By pushing the tail of the injected contrast medium bolus, a saline chaser prevents pooling of contrast material in the peripheral venous compartment at the injection site and in the injection tubing, increasing the effectiveness of contrast material utilization [3]. The increased efficiency provided by a saline chaser can be exploited clinically to: (*i*) decrease the volume of contrast material (typically by 20–30 mL) without jeopardizing vascular and parenchymal enhancement [4–9], (*ii*) increase the magnitude of enhancement (by 5%–10%) using a standard dose of contrast material [10–12] or (*iii*), as recently advocated [13], attain durable and uniform peak enhancement during the entire CT acquisition. However,

although the advantages of a saline chaser for optimizing CT contrast enhancement are widely accepted, disagreement remains over the most effective injection protocol for the administration of saline [14–16]. This uncertainty is compounded by the fact that previous studies analyzed only simulated contrast enhancement in the thoracic aorta using different physiological flow phantoms, with no data regarding enhancement of abdominal parenchymal organs and lack of in vivo validation.

With the widespread dissemination of volume MDCT systems (detector widths up to 16 cm with a collimation of 320×0.5 mm), accurate planning of contrast material injection protocols and precise timing of image acquisition have become crucial to match the extraordinarily narrow imaging window of a clinical CT acquisition (less than 5 s for 300 mm of coverage). We postulate that a thorough understanding of the clinical effects of a saline chaser on vascular and parenchymal contrast medium enhancement could lead to standardized injection protocols, enhanced diagnostic efficiency, and improved patient care.

The purpose of this trial was to prospectively investigate the effect of varying the injection flow rates of a saline chaser on the magnitude, time-to-peak, and duration of both vascular and parenchymal contrast enhancement during abdominal MDCT.

## Materials and methods

One author of the study (RCN) was a medical consultant and a second author (DM) was a research fellow for Bracco Diagnostic, Inc. A third co-author (AG), who is not an employee of or consultant for Bracco Diagnostic, Inc., controlled inclusion of any data or information that might present a conflict of interest.

This prospective, single-center, randomized study was approved by our institutional review board. All subjects provided written informed consent before participating in the study. Patients were informed of the general purpose of the study. They were also told that study participation would entail an approximately 5% increase in radiation dose compared with a standard CT study of the abdomen and pelvis (dose length product, 1,605 mGy•cm vs. 1,527 mGy•cm), but that study participation would not compromise the diagnostic value of the CT examination.

### Study participants and randomization

Patients were eligible for enrollment if they (*i*) were referred clinically for contrast-enhanced MDCT of the abdomen and pelvis, (*ii*) had a pathologically proven primary extrahepatic tumor, and (*iii*) were known or suspected of having metastatic liver disease on the basis of the results of a previous imaging study (ultrasound, contrast-enhanced MDCT, or magnetic resonance (MR) imaging) and/or an increased serum level of carcinoembryonic antigen (>10 ng/mL), prostate-specific antigen (>4.0 ng/mL), or cancer antigens 125 (>30 U/mL) or 19–9 (>15 U/mL). Patients were considered ineligible for the study if they were younger than 18 years old, were pregnant or lactating, had a history of cirrhosis, fatty liver disease, or glycogen storage disease, had a documented decrease in the left ventricular ejection fraction (≤0.50), or had any contraindication to iodinated contrast material, such as a previous history of anaphylactoid reaction, multiple myeloma, organ transplantation, or renal failure (defined as serum creatinine level greater than 2.0 mg/dL [177 μmol/L]). Patients were also deemed ineligible if they were known to have or suspected of having hypervascular liver metastases from melanoma, pancreatic islet cell tumor, thyroid carcinoma, or renal cell carcinoma because the study protocol did not include an entire liver acquisition during the hepatic arterial dominant phase (see, MDCT Technique).

Between November 2008 and March 2009, 100 consecutive patients (mean age, 62 years; age range, 23–86 years), including 59 men (mean age, 63 years; range, 23–86 years) and 41 women (mean age, 60 years; range, 37–80 years), met our inclusion criteria and were prospectively enrolled in the study. After patients were deemed eligible for the study, they were randomly assigned to one of four protocols with different injection flow rates of a saline chaser. Randomization was performed in a 1:1:1:1 ratio. Protocol A, our control group, received an intravenous (IV) injection of 150 mL non-ionic, low-osmolar, monomeric contrast medium. An iodine concentration of 300 mg I/mL (Iomeron 300®; Bracco Diagnostic Imaging, Inc., Princeton, NJ, USA) was delivered at 4 mL/s, with no saline chaser (total iodine dose, 45 g I; total injection duration, 37.5 s; iodine delivery rate, 1.2 g I/s). Protocols B, C, and D underwent the same contrast medium injection scheme as Protocol A, followed by a standard bolus of 50 mL of saline (0.9% sodium chloride, Becton Dickinson, Franklin Lakes, NJ, USA) at injection flow rates of 2 mL/s, 4 mL/s, and 8 mL/s, respectively. This resulted in total "effective" injection durations of 62.5 s, 50.0 s, and 43.8 s for Protocols B, C, and D, respectively. The volume of saline was selected taking into account the average volume of contrast material that remains trapped in the peripheral venous compartment between the injection site and the right atrium of the heart (approximately 40 mL in a normal-sized adult), plus the additional volume of the coiled tubing and IV angiocatheter (approximately 5 mL) [15]. Larger volumes of saline were not tested due to the absence of supporting evidence of an incremental benefit on the magnitude and duration of

vascular contrast enhancement [14]. Saline chaser injection flow rates higher than 8 mL/s were not tested because they are not routinely used for MDCT in clinical practice.

Six (6%) of the 100 patients were excluded from the final analysis because of contrast material extravasation (2 in Protocol D and 1 in Protocol C), technical errors during dynamic CT (2 in Protocol A), or inadequate peripheral venous access (1 in Protocol D).

### Injection technique and patient safety

For all patients, contrast medium was administered using a dual-chamber mechanical power injector (Stellant D CT; Medrad, Indianola, PA, USA) through an 18-gauge, 45-mm IV angiocatheter (Becton-Dickinson and Company, Franklin Lakes, NJ, USA) inserted into a right antecubital vein. Immediately before CT data acquisition, the patency of the angiocatheter was tested with a fast manual flush of 10 mL of saline with the patient's arm in the imaging position. For Protocols B, C, and D, the bolus of contrast media was followed by 50 mL of saline at variable injection flow rates depending on the study-protocol assignment. Contrast material was warmed to 37°C, which resulted in a contrast material viscosity of 4.5 mPa·s. Saline as a chaser was administered at room temperature (approximately 20°C).

At the conclusion of the CT examination, patients were questioned about any discomfort at the injection site, and the site was inspected by a nurse or technologist to identify any associated signs and symptoms of contrast material extravasation, e.g., swelling, blistering, decreased pulses. Patients were asked to document their discomfort during and after contrast material injection using a visual analog scale (VAS), where 0 indicates no discomfort and 100 means worst imaginable anxiety, tenderness, or pain [17].

### MDCT technique

Contrast-enhanced MDCT was performed using a 64-section MDCT (Somatom Sensation 64; Siemens Medical Systems, Erlangen, Germany). The system was equipped with flying focal spot technology, which enables acquisition of double projection data for an identical position of the detector by rapid variation of the focal spot position on the anode [18]. All patients underwent CT in the head-first supine position. After acquisition of an antero-posterior digital scout image, and before contrast medium administration, each patient underwent CT data acquisition craniocaudally from the dome of the liver to the iliac crest during a single breath hold at full inspiration (Table 1). After CT data reconstruction, the single transverse image showing the abdominal aorta, liver, and pancreas was identified by a supervising third-year radiology resident (AG). The CT spatial coordinates of this reference image were noted and used for the subsequent dynamic acquisition.

Single-level dynamic CT acquisitions corresponding to the preselected reference image were begun from 6 to 60 s after the start of contrast medium injection and repeated with a 3-s interval. This acquisition scheme resulted in a total of 19 consecutive CT acquisitions at a single upper-abdominal level. Because four contiguous images were reconstructed during each acquisition for each patient, a total of 76 images were obtained during the dynamic CT study. To limit radiation burden, dynamic CT was performed using a low-dose technique—512×512 matrix, 120 kVp, 20 mAs, 0.5 s gantry revolution time. Automatic exposure control system (CARE Dose 4D, Siemens) was not applied during dynamic CT acquisitions. All patients were instructed to hold their breath as long as possible during dynamic imaging and to continue breathing shallowly thereafter.

The single-level, dynamic CT acquisition was followed by a diagnostic, single-breath-hold CT of the abdomen and pelvis, performed during the hepatic venous phase (70 s after initiation of contrast medium injection).

### Quantitative image analysis

Quantitative measurements were performed on a commercially available workstation (Leonardo, Siemens Medical Solutions) by an abdominal radiology fellow with 4 years' experience in gastrointestinal and hepatobiliary imaging (DM). The reader was blinded to the patient's study protocol assignment. After appropriate magnification, mean CT numbers in Hounsfield units (HU) of the abdominal aorta, pancreas, and liver were obtained for each patient by manually placing circular or ovoid regions-of-interest (ROIs) on the images obtained during all acquisitions — i.e., unenhanced, single-level dynamic, and hepatic venous phases.

The attenuation of the suprarenal abdominal aorta was recorded from a single ROI (mean pixel number, 200; range, 100–250 pixels) drawn to encompass at least 90% of the aortic cross-sectional area. Calcifications and soft plaques of the aortic wall were carefully avoided. The attenuation of the pancreas was recorded as the mean of three ROI readings (mean pixel number, 250; range, 100–350 pixels) at the level of the pancreatic head, body, and tail, respectively. Areas of focal changes in parenchymal density, large vessels, pancreatic ducts, and prominent artifacts were carefully avoided. The attenuation of the liver was recorded as the mean of four ROI readings (mean pixel number, 500; range, 450–600 pixels) placed in the anterior and posterior segments of the right hepatic lobe and the

**Table 1** Multi-detector row CT imaging parameters, reconstruction algorithm, and radiation dose

| CT parameters | Precontrast CT | Single-level dynamic CT[a] | Hepatic venous phase CT |
|---|---|---|---|
| Detector configuration (mm) | 64×0.6 (32×2) | 64×0.6 (32×2) | 64×0.6 (32×2) |
| Peak kilovoltage (kVp) | 120 | 120 | 120 |
| Gantry revolution time (s) | 0.5 | 0.5 | 0.5 |
| Tube current-time product (mAs) | 160 | 20 | 250 |
| Acquisition mode | Helical | Axial | Helical |
| Beam pitch | 1 | N/A | 1 |
| Imaging time (s) | 4–7 | 0.5 | 10–15 |
| Reconstructed section thickness (mm) | 5.0 | 7.2 | 3.0 |
| Field of view (cm) | 35–50 | 35–50 | 35–50 |
| Reconstruction kernel | Soft-tissue (B 20) | Soft-tissue (B 20) | Soft-tissue (B 20) |
| Dose-length product (mGy•cm) | 348 | 74 | 1179 |

[a] Single-level, real-time, dynamic CT was repeated from 3 to 60 s after the start of contrast medium injection, with a 3-s interval, for a total of 20 consecutive CT acquisitions

medial and lateral segments of the left hepatic lobe. Areas of focal changes in parenchymal density, large vessels, and prominent artifacts were carefully avoided.

For each patient, the size, shape, and position of the ROIs were kept constant by applying a copy and paste function on the workstation. To ensure consistency, all measurements were repeated on four consecutive CT sections and the average values were calculated. Manual adjustment of an ROI's location was necessary in 15 patients to correct for subtle changes in the target organs' position because of the patient's breathing.

### Contrast enhancement analysis

For each patient, a time-enhancement curve was generated for the abdominal aorta, pancreas, and liver by plotting the relative enhancement of each organ — expressed as the absolute change in CT numbers (ΔHU) between the unenhanced and each contrast-enhanced acquisition — as a function of time. Time-enhancement curves were analyzed to determine the following previously described enhancement parameters [14–16]: peak enhancement (HU), time-to-peak enhancement (s), and duration of 90% peak enhancement (s). Because the peak enhancement plateau of the liver generally exceeds the 70-second temporal window of our CT acquisition, the duration of 90% peak hepatic enhancement could not be included in the contrast enhancement analysis of the liver.

### Statistical analysis

Baseline demographic and clinical characteristics (age, gender, weight, body mass index, creatinine function), frequency of contrast material extravasations, VAS scores of patient discomfort, and indications for CT imaging were compared among the four randomized protocols using the F-test for continuous variables and Chi-squared test for categorical variables. F-test for comparisons among the four protocols as well as pairwise comparisons between any two protocols were carried out using general linear model (GLM) analysis for peak, time-to-peak, and duration of 90% of peak enhancement for the aorta, pancreas, and liver. The Pearson product-moment correlation coefficient ($r$) was used to assess the correlation between time-to-peak enhancement of the aorta, pancreas, and liver. Linear regression analyses were carried out to determine the linear relationship of time-to-peak enhancement of the aorta on time-to-peak enhancement of the pancreas and time-to-peak enhancement of the liver, respectively.

All statistical analyses were performed with a statistical software package (SAS® 9.0 Software, Cary, NC, USA). A two-sided P value of less than 0.05 was considered to indicate statistical significance.

## Results

### Study participants

There was no statistically significant difference among Protocols A, B, C, and D in baseline demographic or clinical characteristics, general indications for CT imaging, and contrast material extravasation rates (Table 2). The VAS score for patient discomfort during contrast material injection was significantly higher ($P$=0.01 for all comparisons) for Protocol D (mean score, 50.5; range, 20–80) than Protocol A (mean score, 31.5; range, 15–50), Protocol B (mean score, 30.8; range, 10–50), or Protocol C (mean score, 31.8; range, 20–45). There was no statistically significant difference in VAS scores among Protocols A, B, and C. Commonly reported causes of discomfort included unpleasant feeling of warmth (40%, 40 of 100 subjects), pain at the site of injection (10%, 10 of 100 subjects), or both (20%, 20 of 100 subjects).

**Table 2** Demographic and clinical characteristics, frequency of contrast material extravasation, visual analog scale (VAS) scores, and general indications for CT imaging according to the injection protocol

| | Protocol A *N*=25 | Protocol B *N*=25 | Protocol C *N*=25 | Protocol D *N*=25 | All patients *N*=100 |
|---|---|---|---|---|---|
| Age (Years) | | | | | |
| Mean (SD) | 63.1 (11.7) | 62.5 (9.4) | 62.6 (16.0) | 60.0 (13.6) | 62.0 (12.7) |
| Gender | | | | | |
| Female – no. (%) | 9 (36%) | 11 (44%) | 10 (40%) | 11 (44%) | 41 (41%) |
| Weight (kg) | | | | | |
| Mean (SD) | 71.4 (11.2) | 71.8 (12.9) | 69.0 (10.3) | 66.5 (14.5) | 69.7 (12.3) |
| BMI (kg/m$^2$) | | | | | |
| Mean (SD) | 25.6 (8.1) | 26.0 (8.0) | 24.5 (7.5) | 24.1 (7.6) | 25.1 (7.7) |
| Creatinine (mg/dL) | | | | | |
| Mean (SD) | 1.1 (0.3) | 1.1 (0.3) | 1.0 (0.2) | 1.1 (0.3) | 1.1 (0.3) |
| Frequency of extravasation | | | | | |
| Patients – no. (%) | 0 (0%) | 0 (0%) | 1 (4%) | 2 (8%) | 0 (0%) |
| VAS of discomfort | | | | | |
| Mean (SD) | 31.5 (9.7) | 30.8 (10.2) | 31.8 (7.5) | 50.5 (15.7) | 36.2 (10.8) |
| Indications for CT imaging | | | | | |
| Colon cancer – no. (%) | 13 (52%) | 14 (56%) | 9 (30%) | 11 (44%) | 47 (47%) |
| Lung cancer – no. (%) | 7 (28%) | 7 (28%) | 8 (30%) | 11 (44%) | 33 (33%) |
| Prostate cancer – no. (%) | 1 (4%) | 2 (8%) | 3 (12%) | 0 (0%) | 6 (6%) |
| Other – no. (%) | 3 (12%) | 0 (0%) | 5 (20%) | 3 (12%) | 11 (11%) |

BMI = Body mass index (the weight in kilograms divided by the square of the height in meters).

VAS = visual analog scale, where 0 means no discomfort and 100 means worst imaginable anxiety, tenderness, or pain. There was no statistically significant difference among groups for all tested variables.

## Contrast enhancement parameters

Table 3 provides the descriptive statistics of contrast enhancement parameters and the overall P-value for comparison between the four protocols from the F-test. The pairwise comparisons between the groups were then examined and reported here if the F-test is significant at 0.1.

The time-enhancement curves for the abdominal aorta demonstrated significantly higher peak enhancement for Protocol D (369.5 HU±66.2 [standard deviation]) compared with Protocol A (332.9 HU±57.5; $P$=0.05) or Protocol B (326.0 HU±57.4; $P$=0.02), but no significant difference between Protocols C and D (Fig. 1; Table 3). Compared with Protocol A (36.1 s±5.1), the time-to-peak aortic enhancement was significantly later for Protocol D (42.8 s±3.4; $P$<0.001), Protocol C (41.9 s±6.0; $P$<0.001), or Protocol B (40.2 s±3.5; $P$=0.002). There was no significant difference among protocols in the duration of 90% peak aortic enhancement.

The time-enhancement curves for the pancreas demonstrated significantly higher peak enhancement for Protocols C and D (110.6 HU±19.8 and 110.9 HU± 23.8, respectively) compared with Protocol A (92.5 HU± 30.4; $P$=0.04 and 0.02, respectively), but no significant difference in peak enhancement among Protocols B, C and D (Fig. 1; Table 3). The time-to-peak pancreatic enhancement was significantly later for Protocol D (49.6 s±5.1) compared with Protocol A (45.3 s±4.8; $P$=0.003) or Protocol B (46.6 s±3.6; $P$=0.05). There was no statistically significant difference among protocols in the duration of 90% peak pancreatic enhancement.

The time-enhancement curves for the liver demonstrated no statistically significant difference among protocols in peak enhancement and time-to-peak enhancement (Fig. 1; Table 3).

## Linear regression analysis

There were strong positive correlations between the time-to-peak enhancement of the aorta and that of the pancreas for each protocol ($r$ ranges from 0.55 to 0.83) and a moderately positive correlation between the time-to-peak enhancement of the aorta and that of the liver ($r$ ranges from 0.44 to 0.61) (Fig. 2). The linear regression analyses showed that the time-to-peak enhancement of the aorta was linearly related to that of the pancreas for each protocol, with significant difference among the slopes of the regression lines among the four protocols ($P$=0.05; Fig. 2). The latter result suggests that, for equal time-to-peak aortic enhancement, the injection flow rate of a saline chaser may have a substantial effect on the time-to-peak enhancement of the pancreas.

The time-to-peak enhancement of the aorta was also linearly related to the time-to-peak of the liver. However, the slopes of the regression lines were not significantly different across the four protocols (Fig. 2). The following regression equations indicated the optimal diagnostic delay

**Table 3** Enhancement parameters for the aorta, liver, and pancreas for different injection groups

| Enhancement parameters | Protocol A *N*=25 | Protocol B *N*=24 | Protocol C *N*=23 | Protocol D *N*=22 | *P* value |
|---|---|---|---|---|---|
| Aorta | | | | | |
| Peak enhancement (HU) | 332.9 (57.5) [208.0–418.5] | 326.0 (57.4) [226.9–456.7] | 356.1 (70.6) [255.1–595.7] | 369.5 (66.2) [276.4–546.2] | 0.07 |
| Time-to-peak enhancement (s) | 36.1 (5.1) [24–42] | 40.2 (3.5) [30–48] | 41.9 (6.0) [30–54] | 42.8 (3.4) [33–51] | <0.001 |
| Duration of 90% of peak enhancement (s) | 15.8 (4.8) [3–24] | 7.8 (6.6) [3–24] | 8.5 (5.6) [3–18] | 8.9 (7.0) [3–21] | <0.001 |
| Pancreas | | | | | |
| Peak enhancement (HU) | 92.5 (30.4) [42.2–157.5] | 94.1 (21.4) [47.9–120] | 110.6 (19.8) [84.8–162.9] | 110.9 (23.8) [74.7–155.7] | 0.05 |
| Time-to-peak enhancement (s) | 45.2 (4.8) [36–57] | 46.6 (3.6) [39–54] | 47.8 (3.6) [42–54] | 49.6 (5.1) [42–60] | 0.02 |
| Duration of 90% of peak enhancement (s) | 7.4 (4.0) [3–15] | 7.6 (4.2) [3–18] | 6.2 (3.6) [3–15] | 6.2 (3.4) [3–12] | 0.619 |
| Liver[a] | | | | | |
| Peak enhancement (HU) | 74.7 (23.1) [28.2–127.0] | 71.5 (19.6) [24.7–115.3] | 72.3 (21.9) [13.4–110.4] | 75.1 (27.5) [24.6–143.4] | 0.94 |
| Time-to-peak Enhancement (s) | 60.3 (8.5) [36–70] | 63.0 (7.6) [48–70] | 63.6 (4.7) [48–70] | 64.6 (7.7) [48–70] | 0.266 |

Data are mean values, with standard deviation in parentheses and ranges in brackets. NS = not significant.

[a] The duration of 90% of peak enhancement of the liver could not be determined because of the limited temporal window of the CT acquisition (from 3 to 70 s after the start of contrast material administration).

for imaging during peak pancreatic and hepatic enhancement, respectively:

$$TTP_P = 0.67 \bullet 20.9 + TTP_a seconds$$

$$TTP_L = 0.79 \bullet 31.0 + TTP_a seconds$$

where $TTP_P$ is the time-to-peak enhancement of the pancreas, $TTP_a$ is the time-to-peak enhancement of the aorta, and $TTP_L$ is the time-to-peak enhancement of the liver.

## Discussion

Our results demonstrate that the rapid injection of a saline chaser significantly improves aortic and pancreatic peak contrast enhancement during 64-section MDCT of the abdomen. Using a fixed contrast medium injection protocol, the IV administration of 50 mL of saline at 8 mL/s yielded an increase of 11% (95% CI 0%–22%) and 20% (95% CI 0%–41%) in peak contrast enhancement of the aorta and pancreas, respectively, compared with an injection protocol with no saline chaser. Our clinical data corroborate findings of recent experimental studies [14–16], indicating that a faster injection flow rate of a saline chaser improves the magnitude of vascular contrast enhancement during MDCT of the abdomen. In our study, a saline chaser did not increase peak hepatic enhancement compared with a contrast medium injection protocol with no saline chaser.

Another important result of our study, which compares favorably with recent observations [4, 11, 14–16], was a significant delay in time-to-peak aortic enhancement using a saline chaser, with a similar trend for the time-to-peak enhancement of the pancreas and liver. This effect may be explained by longer effective injection duration due to the slightly greater volume of contrast medium pushed by a saline flush. Evidence indicates that injection duration, more than contrast material transit time, has a major impact on time-to-peak contrast enhancement for injection protocols with relatively long injection duration (≥15 s) [19]. To obtain precise imaging acquisition during peak contrast enhancement, our results emphasize the importance of selecting slightly longer imaging delays using a saline chaser. This adjustment may substantially improve the effectiveness of injection protocols required to match the narrower imaging window of faster MDCT systems [16].

Our clinical data demonstrated a strongly positive correlation between the time-to-peak enhancement of the aorta and that of the pancreas. A similar, though less robust, correlation was observed between the time-to-peak enhancement of the aorta and that of the liver. Although our

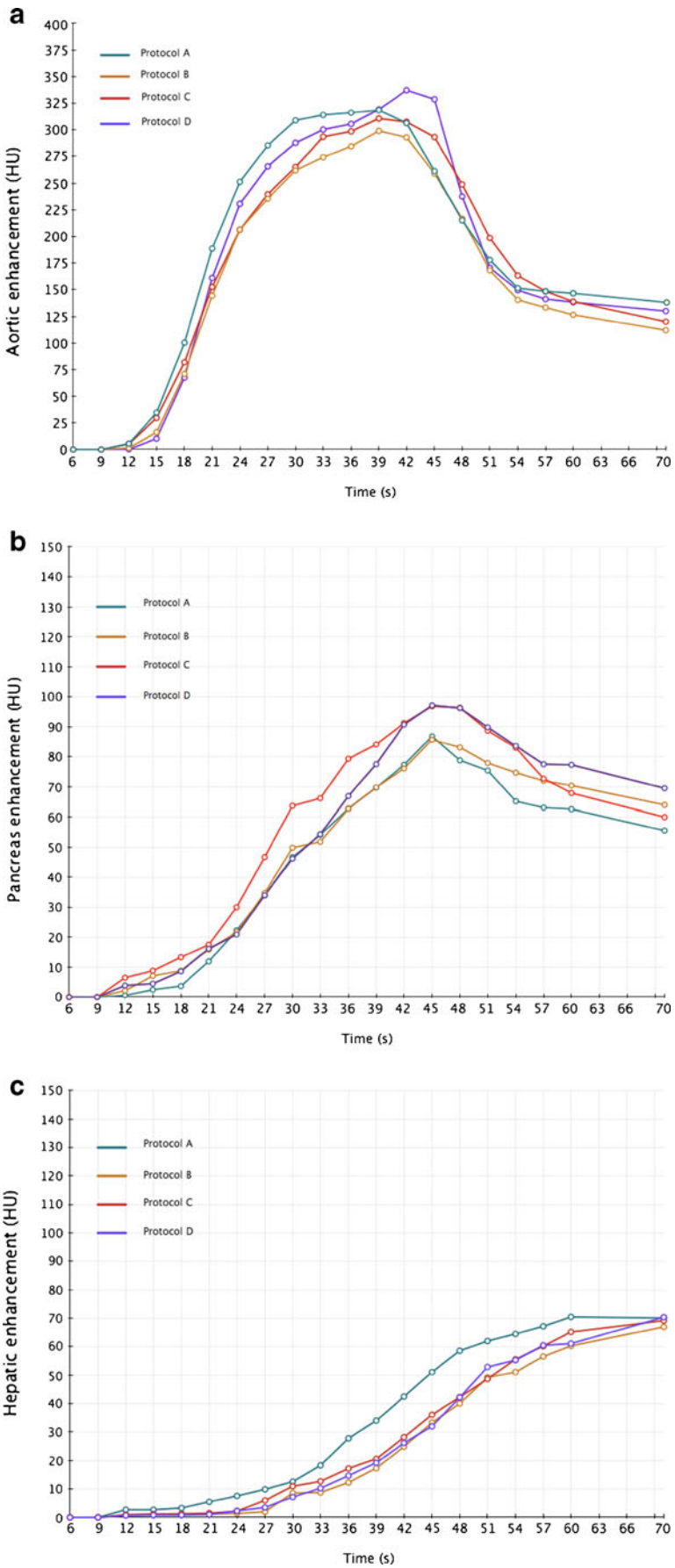


**Fig. 1** Time-enhancement curve diagrams for Protocols A, B, C, and D illustrate the effect of varying the injection flow rates of a saline chaser on the magnitude, time-to-peak, and duration of contrast enhancement for the aorta, pancreas, and liver. For each organ, there was a progressive increase in peak enhancement and slight delay in time-to-peak enhancement, with increasingly higher saline injection flow rates

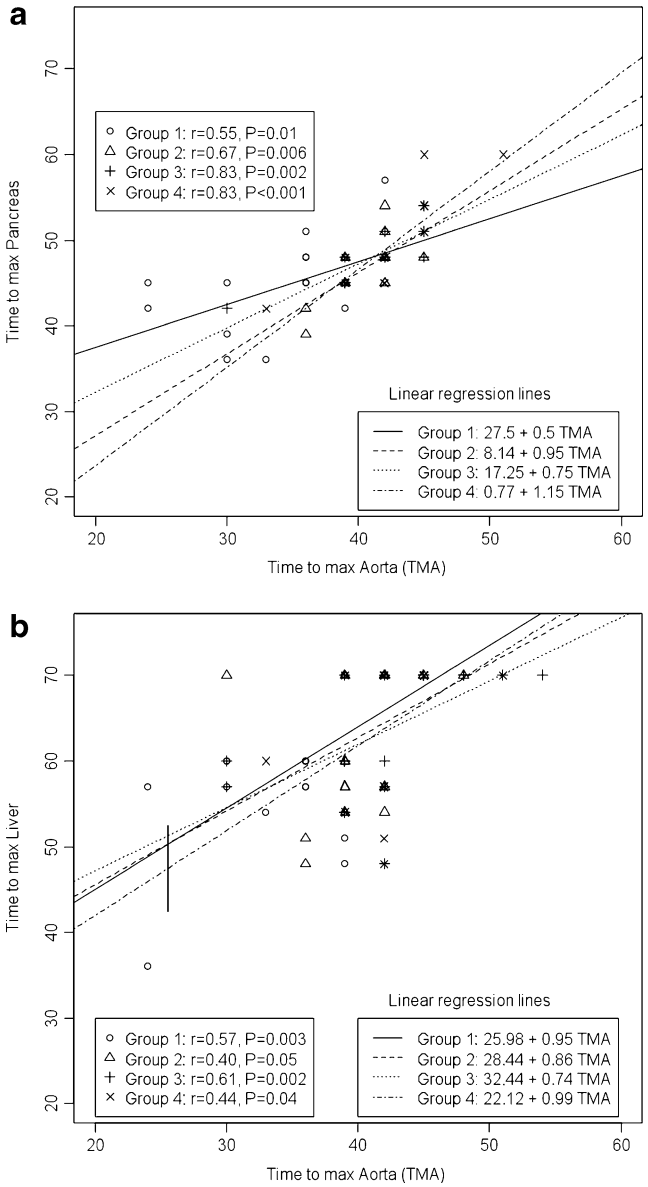


**Fig. 2** Graphs show the relationship between time-to-peak aortic and pancreatic or hepatic enhancement for each injection protocol. **a** There was a strong positive correlation between the time-to-peak enhancement of the aorta and that of the pancreas (*r* ranges from 0.55 to 0.83), with a significant difference in the slopes of the regression lines. **b** There was a moderately positive correlation between the time-to-peak enhancement of the aorta and that of the liver (*r* ranges from 0.44 to 0.61), with no significant difference in the slopes of the regression lines

results are in general agreement with the study by Chu and colleagues [20], there are some marginal differences between our data and Chu's findings. Such discrepancy could have resulted from the difference in temporal resolution for the dynamic acquisition (3 s vs. 1 s, respectively), imaging technique (MDCT vs. MR imaging), and, perhaps more importantly, volume (150 mL vs. 5 mL) and duration (35 s vs. 2.5 s) of contrast medium injection. In agreement with Chu's study [20], we believe that a better understanding of the relationship between time-to-peak aortic and parenchymal organ enhancement is warranted, given the large interpatient variability in peak enhancement intervals. For example, while time-to-peak enhancement occurred, on average, 8 s and 24 s after the time-to-peak aortic enhancement for the pancreas and liver, respectively (which is in agreement with previously published data [21–24]), we found greater variability among individual patients (ranging from 3 to 21 s for the pancreas and 6 to 40 s for the liver depending on the injection protocol). This large variability may explain why suboptimal peak contrast enhancement of abdominal organs may sometimes still be observed with either test bolus or bolus tracking methods [25, 26]. We postulate that a predictive instrument (e.g., a nomogram) for determining peak pancreatic and hepatic enhancement based on time-to-peak aortic enhancement would allow selection of patient-specific rather than fixed diagnostic intervals, ensuring more accurate imaging during peak parenchymal organ enhancement.

Although a saline injection flow rate of 8 mL/s yielded significantly higher patient discomfort (37% increase in VAS score compared with the injection protocol with no saline chaser), including an unpleasant feeling of warmth or pain at the site of injection, there was no significant increase in the frequency of contrast material extravasations at higher saline injection flow rates. Our preliminary findings corroborate the results of previous observations, which showed no correlation between the rate of contrast material administration and the frequency and volume of contrast extravasations using injection flow rates of 0.5–8 mL/s [27–29]. Further data are needed, however, before the use of saline injection flow rates greater than 5 mL/s can be endorsed in patients (*i*) with increased risk of extravasations, such as infants and children, the elderly, or unconscious patients, all of whom may not be able to complain of pain, (*ii*) who underwent multiple attempts to establish an IV access, or (*iii*) in whom only small superficial veins on the dorsum of the hand or foot were readily accessible for puncture [30, 31].

Some potential limitations of our study merit consideration. First, the number of patients in each injection protocol was small thus our findings should be considered preliminary. Second, our results are based on comparisons between different patient groups, and are thus liable to potential confounding due to interpatient variability. Although we found no significant difference among the four protocols for a large number of demographic and clinical characteristics, other confounding factors — most notably, cardiac output and cardiovascular circulation — were not taken into account and could have contributed to observed differences in magnitude or timing of contrast enhancement. Third, it remains to be determined whether the

improved peak aortic and pancreatic enhancement achieved with higher injection flow rates of saline leads to improved diagnostic accuracy or reader's confidence for the detection of vascular and parenchymal abdominal disease.

In conclusion, our preliminary results suggest that the IV administration of a saline chaser using a high injection flow rate (4 or 8 mL/s) yields improved pancreatic and aortic peak contrast enhancement during 64-section MDCT of the abdomen. This improvement is accompanied by a slight, though significant, delay in time-to-peak enhancement and increased patient discomfort at 8 mL/s. Varying the injection flow rate of a saline chaser has no effect on either peak or time-to-peak enhancement of the liver.

Based on our clinical data, we believe a saline chaser using injection flow rates of 4 mL/s or higher should be an important component of CT injection protocols for the abdomen and pelvis, particularly when using faster MDCT systems.

## References


1. Bae KT (2010) Intravenous contrast medium administration and scan timing at CT: considerations and approaches. Radiology 256:32–61
2. Takao H, Nojo T, Ohtomo K (2009) Use of a saline chaser in abdominal computed tomography: a systematic review. Clin Imaging 33:261–266
3. Hopper KD, Mosher TJ, Kasales CJ, TenHave TR, Tully DA, Weaver JS (1997) Thoracic spiral CT: delivery of contrast material pushed with injectable saline solution in a power injector. Radiology 205:269–271
4. Irie T, Kajitani M, Yamaguchi M, Itai Y (2002) Contrast-enhanced CT with saline flush technique using two automated injectors: how much contrast medium does it save? J Comput Assist Tomogr 26:287–291
5. Dorio PJ, Lee FT Jr, Henseler KP et al (2003) Using a saline chaser to decrease contrast media in abdominal CT. AJR Am J Roentgenol 180:929–934
6. Haage P, Schmitz-Rode T, Hübner D, Piroth W, Günther RW (2000) Reduction of contrast material dose and artifacts by a saline flush using a double power injector in helical CT of the thorax. AJR Am J Roentgenol 174:1049–1053
7. Schoellnast H, Tillich M, Deutschmann HA et al (2003) Abdominal multidetector row computed tomography: reduction of cost and contrast material dose using saline flush. J Comput Assist Tomogr 27:847–853
8. Utsunomiya D, Awai K, Tamura Y et al (2006) 16-MDCT aortography with a low-dose contrast material protocol. AJR Am J Roentgenol 186:374–378
9. de Monyé C, Cademartiri F, de Weert TT, Siepman DA, Dippel DW, van Der Lugt A (2005) Sixteen-detector row CT angiography of carotid arteries: comparison of different volumes of contrast material with and without a bolus chaser. Radiology 237:555–562
10. Schoellnast H, Tillich M, Deutschmann HA et al (2004) Improvement of parenchymal and vascular enhancement using saline flush and power injection for multiple-detector-row abdominal CT. Eur Radiol 14:659–664
11. Lee CH, Goo JM, Bae KT et al (2007) CTA contrast enhancement of the aorta and pulmonary artery: the effect of saline chase injected at two different rates in a canine experimental model. Invest Radiol 42:486–490
12. Kim DJ, Kim TH, Kim SJ et al (2008) Saline flush effect for enhancement of aorta and coronary arteries at multidetector CT coronary angiography. Radiology 246:110–115
13. Kubo S, Tadamura E, Yamamuro M et al (2006) Thoracoabdominal-aortoiliac MDCT angiography using reduced dose of contrast material. AJR Am J Roentgenol 187:548–554
14. Behrendt FF, Bruners P, Keil S et al (2010) Effect of different saline chaser volumes and flow rates on intravascular contrast enhancement in CT using a circulation phantom. Eur J Radiol 73:688–693
15. Schindera ST, Nelson RC, Howle L, Nichols E, DeLong DM, Merkle EM (2008) Effect of varying injection rates of a saline chaser on aortic enhancement in CT angiography: phantom study. Eur Radiol 18:1683–1689
16. Coursey CA, Nelson RC, Weber PW et al (2009) Contrast material administration protocols for 64-MDCT angiography: altering volume and rate and use of a saline chaser to better match the imaging window–physiologic phantom study. AJR Am J Roentgenol 193:1568–1575
17. Ripamonti CI, Brunelli C (2009) Comparison between numerical rating scale and six-level verbal rating scale in cancer patients with pain: a preliminary report. Support Care Cancer 17:1433–1434
18. Prokop M (2005) New challenges in MDCT. Eur Radiol 15:E35–E45
19. Bae KT (2003) Peak contrast enhancement in CT and MR angiography: when does it occur and why? Pharmacokinetic study in a porcine model. Radiology 227:809–816
20. Chu LL, Joe BN, Westphalen AC, Webb EM, Coakley FV, Yeh BM (2007) Patient-specific time to peak abdominal organ enhancement varies with time to peak aortic enhancement at MR imaging. Radiology 245:779–787
21. Bae KT, Heiken JP, Brink JA (1998) Aortic and hepatic peak enhancement at CT: effect of contrast medium injection rate—pharmacokinetic analysis and experimental porcine model. Radiology 206:455–464
22. Goshima S, Kanematsu M, Kondo H et al (2006) Pancreas: optimal scan delay for contrast-enhanced multi-detector row CT. Radiology 241:167–174
23. Kondo H, Kanematsu M, Goshima S et al (2007) MDCT of the pancreas: optimizing scanning delay with a bolus-tracking technique for pancreatic, peripancreatic vascular, and hepatic contrast enhancement. AJR Am J Roentgenol 188:751–756
24. Kanematsu M, Goshima S, Kondo H et al (2005) Optimizing scan delays of fixed duration contrast injection in contrast-enhanced biphasic multidetector-row CT for the liver and the detection of hypervascular hepatocellular carcinoma. J Comput Assist Tomogr 29:195–201
25. Itoh S, Ikeda M, Achiwa M, Satake H, Iwano S, Ishigaki T (2004) Late-arterial and portal-venous phase imaging of the liver with a multislice CT scanner in patients without circulatory disturbances: automatic bolus tracking or empirical scan delay? Eur Radiol 14:1665–1673
26. Sandstede JJ, Tschammler A, Beer M, Vogelsang C, Wittenberg G, Hahn D (2001) Optimization of automatic bolus tracking for timing of the arterial phase of helical liver CT. Eur Radiol 11:1396–1400
27. Wienbeck S, Fischbach R, Kloska SP et al (2010) Prospective study of access site complications of automated contrast injection with peripheral venous access in MDCT. AJR Am J Roentgenol 195:825–829

28. Federle MP, Chang PJ, Confer S, Ozgun B (1998) Frequency and effects of extravasation of ionic and nonionic CT contrast media during rapid bolus injection. Radiology 206:637–640
29. Jacobs JE, Birnbaum BA, Langlotz CP (1998) Contrast media reactions and extravasation: relationship to intravenous injection rates. Radiology 209:411–416
30. Wang CL, Cohan RH, Ellis JH, Adusumilli S, Dunnick NR (2007) Frequency, management, and outcome of extravasation of non-ionic iodinated contrast medium in 69,657 intravenous injections. Radiology 243:80–87
31. Nelson RC, Anderson FA Jr, Birnbaum BA, Chezmar JL, Glick SN (1998) Contrast media extravasation during dynamic CT: detection with an extravasation detection accessory. Radiology 209:837–843